Robotica (2014) volume 32, pp. 851–865. © Cambridge University Press 2013
doi:10.1017/S0263574713001045

# Dynamic bipedal walking of a dinosaur-like robot with an extant vertebrate's nervous system

Yasuhiro Fukuoka†* and Junki Akama‡

†*Department of Intelligent Engineering, College of Engineering, Ibaraki University, 4-12-1 Nakanarusawa-cho, Hitachi-shi, Ibaraki 316-8511, Japan*
‡*Seiko Epson Corporation, 80 Hirookaharashinden, Shiojiri-shi, Nagano 399-0785, Japan*

(Accepted October 29, 2013. First published online: December 5, 2013)

**SUMMARY**
In this study, we attempt to develop a biped dinosaur-like walking robot by focusing on its nervous system as well as its mechanism. We developed a robot 'Dinobot' on the basis of palaeontological knowledge on dinosaurs and extant animals. In addition, we employed typical biologically inspired walking gait generation and control methods derived from an extant vertebrate's nervous system. In particular, we utilized a central pattern generator (CPG), which is a locomotion rhythm generator in a vertebrate's spinal cord, to generate the robot's walking rhythm. Moreover, a reflex centre was placed below CPG and it produced joint torque of the legs in the swing and stance phases. Thus, we successfully achieved adaptive 3D dynamic walking generated by the interaction between the original mechanism of dinosaurs and the nervous system of extant animals. Our future goal is to find out a dinosaur's robust locomotive nervous system suitable for its mechanism.

KEYWORDS: Biped robot; 3D dynamic walking; Dinosaur-like robot; Central pattern generator; Limit cycle walking.

## 1. Introduction

A number of researchers have studied the walking or running of a dinosaur using simulation models[41] and robots.[6,22,45] Their mechanisms are built on the basis of palaeontology, in which skeletal specimens are investigated. On the other hand, to produce their gaits, various control methods have been heuristically tried. However, the simulation models are limited in the sagittal plane, and the robots walk slowly and cannot adapt to any perturbation.

In the field of biomechanics, Sellers *et al.*[41] developed dinosaur running simulation models for estimating the maximum running speed of dinosaurs. For the design of the running mechanism, the segment properties of limbs, muscles and tendons are derived from previous findings on dinosaurs, extant animals and humans. On the other hand, for producing their walking gaits, the gait cycle duration and the muscle activation levels are optimized by a genetic algorithm. It runs only on flat terrain in the sagittal plane. In the robotics field, Hirukawa *et al.*[22] built a dinosaur robot with joint configuration and link length based on skeletal specimens of dinosaurs. For producing its walking gait, it utilizes a motion control method based on a zero-moment-point (ZMP) stability criterion peculiar to conventional walking robots. Dilworth[6] developed the robot 'Troody' according to the skeletal model of Troodon, which inhabited North America in the late Cretaceous period. For walking gait generation, the desired trajectories are produced on the basis of the ZMP-based locomotion control method as in Hirukawa *et al.*[22] Takita *et al.*[45] developed a small dinosaur-like robot 'TITRUS'. The gait was generated by trial and error, and walking with quick short steps was achieved by actively swinging its head and tail. However, these robots' walking speeds are slow and they do not adapt to disturbance.

As stated above, typically, the mechanism in a dinosaur model, including the joint configuration and link length, is based on the skeletal specimens of dinosaurs. Furthermore, the muscles and

* Corresponding author. E-mail: fukuoka@mx.ibaraki.ac.jp

tendons to drive the joints are modelled on the basis of those of extant vertebrates. However, for gait generation and locomotion control methods, researchers have been seeking a suitable method based on the conventional legged locomotion control or learning methods.

Therefore, we propose employing a legged locomotion generator and controller on the basis of the fundamental dynamic locomotive nervous system of extant vertebrates indicated in biology and neurophysiology. We mounted the system on a biped dinosaur-like robot that has mechanical features described in palaeontology and biomechanics. Then we experimentally examined whether the robot could accomplish stable walking, and possessed flexible autonomous adaptability to disturbance while walking. As a result, dynamic walking was achieved and the robot could ever autonomously adapt to the situation in which an unperceived step appeared on flat terrain.

Our future goal is to find out a dinosaur's robust locomotive nervous system suitable for its mechanism. It cannot be explained by analysing the skeletal specimens alone. The evaluation is extremely difficult because dinosaurs are extinct species, but we intend to validate our system by demonstrating the robot's walking stability and adaptability to disturbance, which are essential to an extant animal's locomotion. We hope that our results will finally contribute to understanding the walking dynamics of dinosaurs in palaeontology.

This paper is organized as follows. In Section 2 we explain an extant animal's nervous system for dynamic walking. In Section 3 we introduce the mechanical design of our biped dinosaur-like robot. Section 4 describes the walking gait generation and control. Section 5 summarizes the experimental results of our robot's dynamic walking on both flat and uneven terrains. Finally, Sections 6 and 7 end the paper with discussion and conclusions.

## 2. An Extant Animal's Nervous System for Dynamic Walking

Contemporary biology reports that various animals such as lampreys, which are the oldest extant vertebrates, cockroaches, leeches, lobsters and even cats have a locomotion rhythm generator in their spinal cord.[5, 18, 37, 42, 43] The generator is called central pattern generator (CPG). CPG is also capable of autonomously adapting to changeable and unpredictable states of walking through a combination of spinal reflexes.[5, 7, 18, 37] Therefore, we considered that because dinosaurs are regarded as vertebrates, they could have been equipped with a basic nervous system for walking that is still possessed by extant animals. We decided to exploit CPG and spinal reflexes for our gait generation and control system.

Taga *et al.*[44] constructed CPG and a spinal reflexes model for a biped simulation model and successfully achieved dynamic walking in the sagittal plane of the model. They state that dynamic walking is not a simple behaviour generated by the movement of an individual body but is a complicated nonlinear dynamic phenomenon that produces limit cycles by mutual entrainment between a body and the environment. Following their work, a number of biologically inspired biped robots that employ CPG or similar oscillators have successfully achieved planar dynamic walking in the sagittal plane[8, 24, 29, 33, 46] and 3D dynamic walking.[1, 9, 28] All the planar bipeds are capable of walking with high speed with small feet and long steps,[8, 24, 29, 33, 46] but all the 3D bipeds possess large feet and short steps to keep their balance, and their speeds are slow.[1, 9, 28] Currently, it is difficult for a biped robot adopting the biologically inspired method with CPG to 3D walk at high speed with much longer steps than its foot length and adapt to perturbations of humans and animals. However, a bird and a biped dinosaur having a levelled trunk with a head and a tail implicitly involve an inherent mechanical stable element to keep their balance (Section 3). Our aim is to determine a dinosaur's robust locomotion nervous system as we have mentioned earlier; we can also expect that a biped dinosaur-like robot can walk 3D with small feet and long steps depending on a simple walking rhythm generation by CPG and reflexes.

In biomechanics, Full *et al.*[15] stated that posture control at the brain level is required in low-speed walking, whereas self-stabilization depending on the spring-damper characteristics of muscles and tendons is dominant in high-speed walking and running. In addition, they showed that CPG and reflexes work effectively in the medium-speed range. Because we intend to design a gait generation and control system with CPG and reflexes, we aim to realize medium-speed walking with a Froude number of approximately 0.6. (The Froude number ($Fr$) is a dimensionless criterion to evaluate the mobile speed of a body regardless of its size.[2] It is given by $Fr = v/\sqrt{gl}$, where $v$, $g$ and $l$ denote speed, gravitational acceleration and leg length, respectively.)

https://doi.org/10.1017/S0263574713001045 Published online by Cambridge University Press

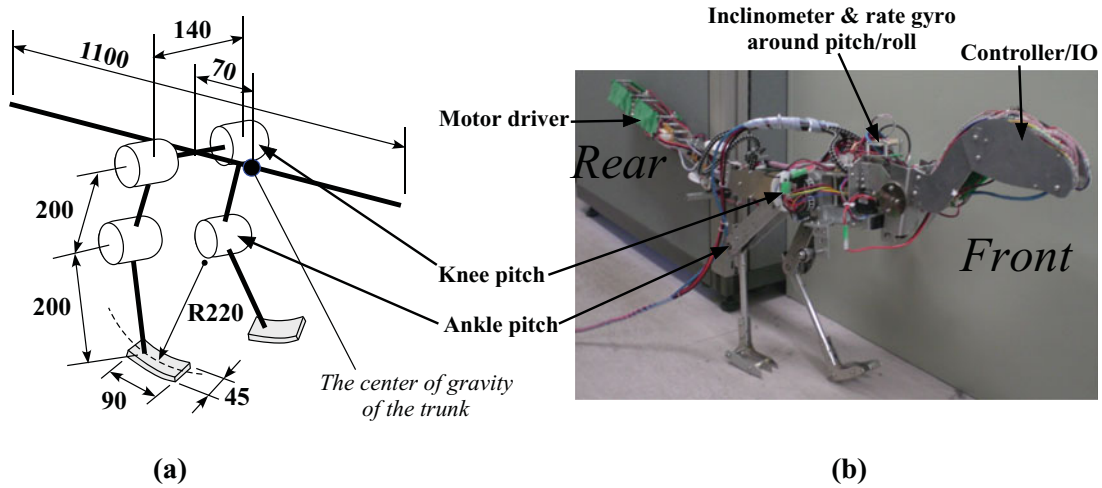


Fig. 1. (Colour online) (a) The joint configuration, and (b) photo of the dinosaur-like robot 'Dinobot'. Dinobot is tethered to a power supply. Dinobot weighs 4.3 kg (each leg: 380 g, the trunk including the head: 2840 g, the tail: 700 g) with a length of 1.1 m and a height of 0.55 m. The moment of inertia of the trunk around the centre of gravity around the yaw axis is 0.268 kg $m^2$. The leg length is 0.4 m and the distance between the two knee joints is 0.14 m. Each foot part is a single rigid body of 90-mm length, 45-mm width and 220-mm curvature radius. Each joint is driven by a DC motor (Maxon Co. RE25: 20W). The reduction gear mechanism is assembled by spur gears and has a small viscous friction, and the reduction ratio of the knee and ankle joints is 40:1. An encoder with a DC motor measures the joint angle. In addition, the body inclination is measured using a piezoelectric vibrating gyroscope (Murata Co. ENC-03R).

## 3. Mechanical Design of the Biped Dinosaur-Like Robot

We developed a biped dinosaur-like robot that we called 'Dinobot'. Figure 1 shows the robot with its specifications. Dinobot was modelled on 'Compsognathus',[27] which is a small bipedal theropod dinosaur of approximately 1-m length. In terms of Dinobot's leg structure, a general bipedal theropod's leg consists of three main long bones, which are the femur (i.e., the part between the hip and the knee), the tibia (i.e., the part between the knee and the ankle) and the tarsus (i.e., the part between the ankle and upper part of the foot).[13] Dinobot does not have the femur segment; i.e, Dinobot has only two joints (knee and ankle joints) around the pitch axis in each leg. However, Compsognathus's leg structure is very similar to that of birds', which evolved from dinosaurs,[27] such as other bipedal theropods, and birds also have an immobile femur segment (the hip is statically buried in the torso) and a mobile posterior tibia and almost vertical tarsus. This is similar to Dinobot's leg structure. The ratio of the lengths of the tibia, the tarsus, the tail and the torso along with the head were determined based on the specimen of Compsognathus.[35]

In biomechanics, Full *et al.*[15] stated that running dynamics is simply modelled by the motion of the spring-loaded inverted pendulum (SLIP) model, which is a single degree of freedom (DOF) linear leg composed of a mass and a spring, and Holmes *et al.*[23] reported that relative leg stiffness is very similar in bipeds, quadrupeds and hexapods despite their different leg shapes. Therefore, we consider that an essential factor for dynamic walking is to swing the leg to a valid contact point in the swing phase and to support the body in the stance phase, and reducing the number of leg joints has a negligible influence on the global dynamics of dynamic walking. Therefore, at this stage, we decided to focus on enabling the robot to walk reliably with the lowest possible number of leg joints.

Dinobot's leg joints only revolve around the pitch axis. The end of the femur in the shoulder joint of general bipedal theropods do not form a globular shape like in humans, but a cylindrical shape which restricts the leg motion around the pitch axis.[13] Similarly, the limbs of birds have traditionally been characterized as being restricted to planar motion in the sagittal plane by hinge-like hip, knee and ankle joints.[17]

As it is vital for high-speed animals to agilely swing their legs, birds have light legs to minimize the moment of inertia of the limbs. To mimic these characteristics, actuators that drive all leg joints are placed on the torso by using timing belts and pulleys, and Dinobot is equipped with small feet. Furthermore, as animals' flexible joints are effective for absorbing the shocks transmitted to their

https://doi.org/10.1017/S0263574713001045 Published online by Cambridge University Press

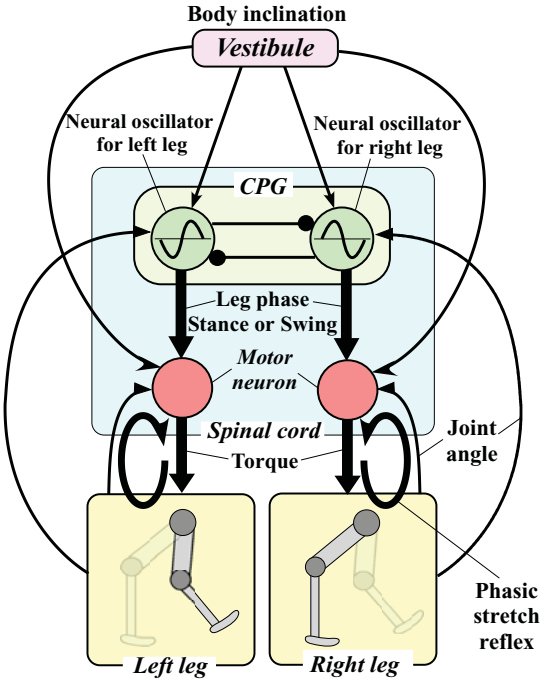


Fig. 2. (Colour online) Dinobot's nervous system composed of CPG, motor neurons and a vestibule. CPG and the motor neurons are located at the higher level and the lower level in the spinal cord, respectively. Each thin arrow from the leg indicates the sensory feedback of a joint muscle's length measured by an angle sensor. Each thin arrow from the vestibule indicates the sensory feedback of body inclination around the pitch and roll axes. In general, CPG produces self-excited oscillations and merely transmits each leg's phase switching signal (swing/stance) to the motor neuron, in which each leg is driven by a PD controller, as described in Section 4.1.2.

feet from the ground while walking, we mimicked the function by using joints with a small viscous friction designed with a low reduction ratio.

A distinct characteristic of biped dinosaurs is the possession of a heavy levelled trunk with head and tail, unlike numerous extant animals. The moment of inertia of a biped dinosaur's tail is much larger than that of birds', which are otherwise structurally similar to dinosaurs. This characteristic is reported by a well-known study on dinosaurs[3] and is considered an effective feature for walking. The existence of the long trunk with a head and a tail and keeping the body level contribute to increasing the moment of inertia of the body around the pitch and yaw axes; in addition, it inhibits vibration of the body while walking. Based on this report, Dinobot is also equipped with a level trunk with a long tail and a head.

It was inferred on general bipedal theropods that the point where each leg was joined was located somewhat behind the centre of gravity on the level trunk,[13] and therefore we attached the legs 70 mm (experimentally determined) behind the centre of gravity of the trunk as shown in Fig. 1.

## 4. Walking Gait Generation and Control

Dinobot employs walking gait generation and control systems based on the biologically inspired method utilized in 'Tekken', which is a quadruped robot developed by Fukuoka *et al.*[12,25] The system is outlined in Fig. 2. Dinobot's walking gait is generated by mutually coupled nonlinear oscillators called neural oscillators. Each oscillator produces the swinging rhythm of a single leg. We call this upper walking gait generation system CPG. The neural oscillator for each leg transmits a leg phase switching signal of a swing/stance phase to each leg. The part that produces the leg joint torque, called the motor neuron, receives the phase switching command, and the leg is controlled differently in the swing and stance phases on the basis of a phasic stretch reflex. [1] The phasic stretch reflex is

[1] A phasic reflex is rapid, brief and involves an intense muscular contraction; in contrast to this, a tonic reflex is long-lived, and is of low intensity.[40]

https://doi.org/10.1017/S0263574713001045 Published online by Cambridge University Press

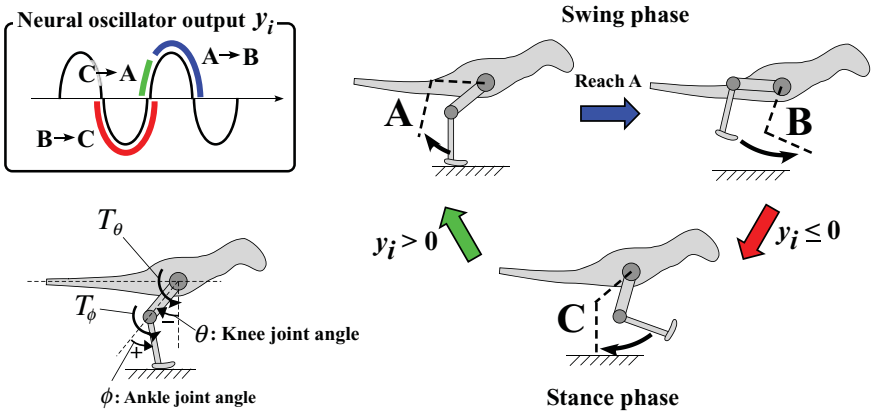


Fig. 3. (Colour online) PD control of each leg by the phasic stretch reflex. The figure on the top left shows a typical neural oscillator's output $y_i$ ($i = 0$: left leg, $i = 1$: right leg). According to $y_i$, each leg is PD-controlled to the three desired leg positions in the order A, B and C, as shown by the broken lines in the right figure, according to Eqs. (4) and (5). For example, in the duration of the bold curve of B→C in the top left figure, the leg is moving from the leg position B to C of the right figure. The figure in the bottom left shows the origin and orientation of the knee $\theta$ and ankle $\phi$ joint angles and the orientation of each torque used in the PD and other controls. The $\theta$ and $\phi$ are relative angles that are measured by encoders. For the sake of simplicity, the other leg is eliminated in these figures, but it is also PD-controlled according to the other neural oscillator output (e.g., $y_1$ if $i = 0$ in these figures).

the most fundamental spinal reflex performed in a muscle,[39] and when muscular tissue is extended from the initial position, it is contracted by the reflex. We set three initial leg positions for the phasic stretch reflex, and the neural oscillator discretely switches each position (Fig. 3). The motor neuron controls the leg towards each leg position in the appropriate order. As a result, Dinobot is capable of producing its leg trajectory for walking. Furthermore, we apply postural reflexes to adjust CPG and the phasic stretch reflex according to the body inclination information obtained from a vestibule.

### *4.1. Walking gait generation and control in the sagittal plane*

In the following Sections (4.1.1–4.1.3), we demonstrate the dynamic walking of Dinobot in the sagittal plain by employing walking gait generation and control around the pitch axis.

*4.1.1. Walking gait generation by CPG.* We use Matsuoka's neural oscillator,[31] which consists of two mutually inhibiting neurons in Dinobot. The oscillator has a specific feature that it synchronizes with external oscillations, such as a sensory input, and can autonomously modulate its own oscillation according to the state, and that it autonomously returns to its usual stable state from temporal disturbance. These features were demonstrated by a number of legged locomotion models and robots (e.g., a monopod hopping robot,[38] biped walking simulations,[21,44] a biped walking robot[30] and a quadruped walking robot[12]) and analyzed by several studies.[26,32,47] Each neuron in the model is represented by the following nonlinear differential equations, based on Matsuoka's oscillator model,[31]

$$\begin{aligned}
\tau \dot{u}_{\{e,f\}i} &= -u_{\{e,f\}i} + w_{fe} y_{\{f,e\}i} - \beta v_{\{e,f\}i} \\
&\quad + u_0 + Feed_{\{e,f\}i} + \sum_{j=1}^{2} w_{ij} y_{\{e,f\}j}, \\
y_{\{e,f\}i} &= \max\,(u_{\{e,f\}i}, 0), \\
\tau' \dot{v}_{\{e,f\}i} &= -v_{\{e,f\}i} + y_{\{e,f\}i},
\end{aligned} \tag{1}$$

where

- the suffixes are defined as follows:
  $e$: an extensor neuron,

https://doi.org/10.1017/S0263574713001045 Published online by Cambridge University Press

$f$: a flexor neuron,
$i$: the number of neural oscillators
(0: for the left leg, 1: for the right leg);

- the variables are defined as follows:
  $u$: the inner state of an excitatory neuron,
  $v$: the inner state of an inhibitory neuron,
  $y$: the output of an extensor/flexor neuron,
  $Feed$: sensory feedback signals from the robot;
- the parameters are defined as follows:
  $\beta$: a constant representing the degree of self-inhibition influence on the inner state,
  $\tau$: the time constant of $u$,
  $\tau$': the time constant of $v$,
  $u_0$: an external input with a constant rate,
  $w_{fe}$: a connecting weight between the extensor and flexor neurons,
  $w_{ij}$: a connecting weight between neurons of the $i$th and $j$th neural oscillator.

This neural oscillator is applied to each leg. The oscillators are mutually connected to each other and generate walking gaits. During walking, the relationship between the oscillations of the two legs is usually in anti-phase. Therefore, each oscillator is inhibitorily coupled, but is under the influence of the sensory feedback $Feed_{\{e,f\}i}$ and the phase difference between the two legs is appropriately adjusted according to the walking state. Thus, Dinobot becomes capable of adapting to the perturbations while walking over irregular terrain. The output of a neural oscillator is shown as follows,

$$y_i = -y_{ei} + y_{fi}, \tag{2}$$

$y_i$ appears to be a sinusoidal wave. If $y_i > 0$, the flexor neuron is activated and the leg is led to the swing phase, and if $y_i < 0$, the extensor neuron is activated and the leg is led to the stance phase. In this manner, each leg phase is switched by the neural oscillator. However, if the leg is merely swung following the rhythm of $y_i$, a deviation between the output and the actual leg motion appears. Therefore, using Eq. (3) together with the sensory information (the knee joint angle $\theta$: the origin and direction are shown in Fig. 3) of each leg, the oscillations of the neural oscillator and the actual leg can be synchronized,

$$\begin{aligned} Feed_{e\cdot tsr} &= k_{tsr}(\theta - \theta_0), \\ Feed_{f\cdot tsr} &= -Feed_{e\cdot tsr}, \\ Feed_{\{e,f\}} &= Feed_{\{e,f\}\cdot tsr}. \end{aligned} \tag{3}$$

This adaptation refers to the tonic stretch reflex (TSR) of animals,[34] which is a reflex to sustain muscle contraction in response to slow stretching. $k_{tsr}$ is the feedback gain and the constant parameter $\theta_0$ represents $\theta$ while standing. The suffix $i$ is eliminated when referring to a single neural oscillator.

*4.1.2. Leg control using the phasic stretch reflex.* As shown in Fig. 2, based on the leg phase switching signal $y_0$ or $y_1$ (Eq. (2)) from each neural oscillator in CPG, each leg is proportional-derivative (PD)-controlled to three separate desired leg positions marked as A, B and C in Fig. 3. First, if $y_i \leq 0$ (stance phase), Dinobot supports its body against gravity and obtains propulsion by treading over the ground (Fig. 3-position C). Second, if $y_i > 0$ (the beginning of the swing phase), Dinobot lifts the leg backward (Fig. 3-position A) so that the toe does not touch the ground while swinging. Finally, if the knee joint angle reaches the desired angle of A within $y_i > 0$, Dinobot swings the leg forward (Fig. 3-position B). These three states sequentially occur according to the rhythmic output from the neural oscillator on each leg, and thus walking motion is produced.

The joint output torque of the knee and ankle joints for each of the three states A, B and C is calculated by the following PD control Eqs. (4) and (5), respectively:

$$T_\theta = k_{ph\{A,B,C\}}(\theta_{d\{A,B,C\}} - \theta) - k_{dh\{A,B,C\}}\dot{\theta}, \tag{4}$$

$$T_\phi = k_{pa\{A,B,C\}}(\phi_{d\{A,B,C\}} - \phi) - k_{da\{A,B,C\}}\dot{\phi}. \tag{5}$$

https://doi.org/10.1017/S0263574713001045 Published online by Cambridge University Press

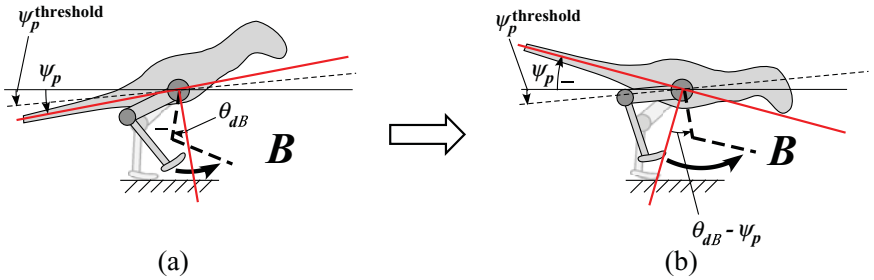


Fig. 4. (Colour online) A stepping reflex for the swing leg is triggered when Dinobot inclines sharply forward. B in these figures refers to the desired position in the swing phase in Fig. 3. $\psi_p$ represents the body inclination. When the trunk is levelled, $\psi_p = 0$ and when it is inclined backward, $\psi_p > 0$. The threshold of the stepping reflex is denoted by $\psi_p^{\text{threshold}}$. Usual walking posture is shown in (a). In (b), the body inclination is beyond the threshold ($\psi_p < \psi_p^{\text{threshold}}$) and Dinobot is about to fall forward. Then, the stepping reflex is activated and Dinobot steps further forward in the swing phase.

For all joints, $T$, $\theta$ (or $\phi$) and $\dot{\theta}$ (or $\dot{\phi}$) are the tension of the joint muscle (joint torque), the current joint muscle length (current joint angle) and the current joint muscle velocity (current joint angular velocity), respectively. Angles $\theta_d$ and $\phi_d$ are the equilibrium values of joint muscle length (desired joint angles). For example, $\theta_{dA}$ is the desired knee joint angle for position A and $\phi_{dB}$ is the desired ankle joint angle for position B. The origin and direction of each angle and the direction of each torque are shown in Fig. 3. The values $k_p$ and $k_d$ are the proportional (P) and derivative (D) gains (e.g., $k_{paA}$ represents the P-gain of the ankle joint for position A). If the muscle is extended from the equilibrium (e.g., $\theta_d$, $\phi_d$), it is contracted by the phasic stretch reflex. This is mimicked by the PD control. Consequently, a typical walking trajectory is produced.

*4.1.3. Postural reflex in the sagittal plane.* At times, the trunk has a tendency to gradually incline even on flat terrain or to suddenly incline the moment the foot stumbles over a step. To avoid falling forward, we apply a stepping reflex[36] in the swing phase to enable posture adaptation, as shown in Fig. 4. In the state A→B in Fig. 3, if the body inclines forward and the inclination $\psi_p$ crosses the threshold $\psi_p^{\text{threshold}}$, as shown in Fig. 4(a) and (b), Dinobot changes the typical desired knee joint angle $\theta_{dB}$ in Fig. 3-position B to $\theta_{dB} - \psi_p$ and steps further forward. As a result, Dinobot can regain its posture after a few steps and avoids falling forward. This reflex has a beneficial effect on the adaptation to disturbance while walking over rough terrain.

### *4.2. Postural reflex in the lateral plane*

Dinobot has joints only around the pitch axis. However, because rolling and yawing motions occur naturally in dynamic walking, we have to consider them.

First, regarding the motion around the yaw axis, the dinosaur's long levelled trunk with head and tail has a large moment of inertia around the yaw axis. As a result, the oscillation of the body around the yaw axis is small and has little influence on walking.

Second, we consider the motion around the roll axis. While dynamically walking on flat terrain with a short cyclic period (approximately 0.4 s), the fluctuation of the angular momentum around the stance leg contact point on the ground is small. Therefore, the rolling oscillation amplitude is also small. However, while walking over irregular terrain, the body often uncontrollably oscillates around the roll axis. Then the phase difference of the oscillation between the legs around the pitch and the body around the roll axis leads to instability. Accordingly, we established Eq. (6) as the feedback to the neural oscillator, and Eq. (7) as the input $Feed_{\{e,f\}i}$ in Eq. (1). As a result, the pitching and rolling motions are mutually synchronized,

$$\begin{aligned} Feed_{e\cdot vsr} &= \delta(\text{leg})\, k_{vsr} \times \psi_r, \\ Feed_{f\cdot vsr} &= -Feed_{e\cdot vsr}, \end{aligned} \tag{6}$$

https://doi.org/10.1017/S0263574713001045 Published online by Cambridge University Press

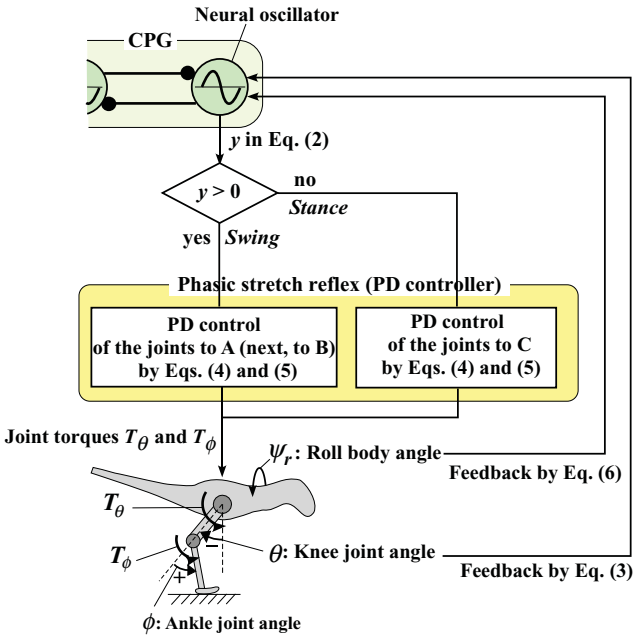


Fig. 5. (Colour online) The diagram shows the control algorithm of each leg. The stepping reflex is eliminated in this figure. The knee and ankle joints are controlled to the leg positions, first to A, then from A to B or to C in the PD controller in Fig. 3 according to the sign of the neural oscillator output $y$. The oscillator receives the sensory feedbacks of the knee joint angle $\theta$ and the roll body angle $\psi_r$.

$$\delta(\text{leg}) = \begin{cases} 1, \text{ if } leg \text{ is a right leg} \\ -1, \text{ otherwise} \end{cases},$$

$$\begin{aligned} Feed_e &= Feed_{e\cdot tsr} + Feed_{e\cdot vsr}, \\ Feed_f &= Feed_{f\cdot tsr} + Feed_{f\cdot vsr}. \end{aligned} \tag{7}$$

This adaptation is based on the vestibular spinal reflex (VSR) of animals,[10] which is the reflex when the head is inclined, a downward-inclined leg is extended and an upward-inclined leg is flexed. This reflex around the roll axis prevents the body from excessively inclining sideways in the lateral plane. Here $k_{vsr}$ is the feedback gain and suffix $i$ is eliminated as in Eq. (3). The body angle around the roll axis is shown as $\psi_r$ in Eq. (6). When standing still, $\psi_r = 0$, and when right inclined, $\psi_r > 0$.

### *4.3. Integration of CPG and reflexes*

The diagram of the control algorithm of each leg described in Sections 4.1 and 4.2 is depicted in Fig. 5 (eliminating the stepping reflex to adapt to disturbance). According to the sign (disregarding the amplitude) of the neural oscillator output $y$ in Eq. (2), the knee and ankle joints are controlled by the PD controller in Fig. 3 using Eqs. (4) and (5) so that the leg reaches the desired leg position of the swing phase (A and B) or the stance phase (C). Therefore, the leg swings following the rhythm of the oscillator ~D. In order to synchronize the neural oscillation, the leg oscillation and the body rolling oscillation while walking, sensory feedbacks of the knee joint angle $\theta$ and the roll body angle $\psi_r$ are delivered to the oscillator through Eqs. (3) and (6). The standard walking cycle duration determined by the oscillator's parameters (e.g., $\tau$ and $\tau'$ in Eq. (1)) is autonomously adjusted by the feedbacks, and thus the oscillator usually produces an adaptive walking rhythm. The two legs are related to each other through only the mutual inhibition between their oscillators. Although the algorithm used for flat terrain walking is simply shown by Eqs. (1)–(7), Dinobot is capable of walking safely on flat terrain by suitably adjusting the timing of the switching of leg phases (swing/stance) without explicitly adjusting the leg trajectories.

https://doi.org/10.1017/S0263574713001045 Published online by Cambridge University Press

Table I. The parameter values used in the experiments. (a) The neural oscillators [Eqs. (1), (3), (6)]. (b) The PD controllers (Fig. 3). All values were determined experimentally.

(a)

| Parameters | Value | Parameters | Value |
|---|---|---|---|
| $u_0$ | 1.0 | $w_{\{11,22\}}$ | 0 |
| $\tau$ | 0.06 | $w_{\{12,21\}}$ | −0.7 |
| $\tau'$ | 0.6 | $k_{tsr}$ (1/rad) | 1.7 |
| $\beta$ | 2.0 | $\theta_0$ (rad) | −0.75 |
| $w_{fe}$ | −1.5 | $k_{vsr}$ (1/rad) | 1.4 |

(b)

| Desired angle | Value (rad) | P-gain | Value (Nm/rad) | D-gain | Value(Nm·s/rad) |
|---|---|---|---|---|---|
| $\theta_{dA}$ | −0.91 | $k_{phA}$ | 2.0 | $k_{dhA}$ | 0.015 |
| $\theta_{dB}$ | −0.37 | $k_{phB}$ | 5.2 | $k_{dhB}$ | 0.01 |
| $\theta_{dC}$ | −0.72 | $k_{phC}$ | 19.5 | $k_{dhC}$ | 0.025 |
| $\phi_{dA}$ | 1.27 | $k_{paA}$ | 6.0 | $k_{daA}$ | 0.005 |
| $\phi_{dB}$ | 1.27 | $k_{paB}$ | 9.0 | $k_{daB}$ | 0.005 |
| $\phi_{dC}$ | 0.38 | $k_{paC}$ | 21.0 | $k_{daC}$ | 0.03 |

## 5. Dynamic Walking Experiment

Neural oscillators are classified as nonlinear oscillators, which have two particular mathematical features as follows.

First, when external oscillations with different frequencies are input to a nonlinear oscillator, it autonomously modulates its own frequency and synchronizes with the external oscillations.[19,20] In Section 5.1, we verify that Dinobot with neural oscillators is capable of stable dynamic walking on flat terrain because of the first feature. This would also determine whether Dinobot's neural oscillators can synchronize their own neural oscillation with the legs' oscillations, the body pitching oscillation and the body rolling oscillation, and whether Dinobot is capable of continuous walking, which means that a limit cycle is constructed.

The other mathematical feature of nonlinear oscillators is self-stabilization, which means that it autonomously returns to its usual stable state in a short time even if it receives temporal disturbance. To prove that our system exhibits this characteristic, we demonstrated that Dinobot did not topple after perturbations caused by walking over a step. This is described in Section 5.2.

The parameter values of the gait generation and control systems used in the experiments in this section are experimentally determined, and are shown in Table I. Note that the values of all parameters for Dinobot are constant. MPEG footage of the walking experiments in this section can be seen at http://fukuoka.ise.ibaraki.ac.jp/.

### *5.1. Walking on flat terrain*

We performed experiments of Dinobot walking on flat terrain. We show snapshots, experimental data and a phase plane trajectory in figure snapshots, experimental data and a phase plane trajectory in Figs. 6–8, respectively. In this experiment, the walking speed was 1.15 m/s, the walking cycle duration was 0.41 s, *Fr* was 0.58 and the step was 0.2 m, which is much longer than the foot length (0.09 m). The duty factor was 0.57, and the number of steps was 20.

In Fig. 7, the neural oscillator's outputs and the knee joint angles are shown as cyclic and organized oscillations. In addition, all oscillations have the same constant cycle duration. This proves that the neural oscillator and the leg movement were synchronized. We can observe that the body inclination around the roll axis $\psi_r$ fluctuates slightly but is stable around 0 rad. Moreover, the body inclination around the pitch axis $\psi_p$ is stabilized around approximately 0.2 rad, which denotes a slight back-inclined posture. As the threshold of the stepping reflex ($\psi_p^{\text{threshold}}$; Section 4.1.3) is empirically set to 0.07, the body pitch inclination $\psi_p$ is always greater than $\psi_p^{\text{threshold}}$. As a result, the stepping reflex was not activated while walking on flat terrain.

https://doi.org/10.1017/S0263574713001045 Published online by Cambridge University Press

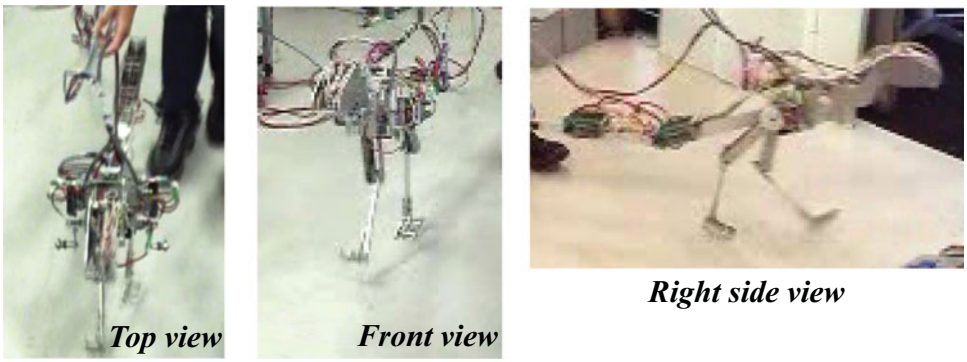


Fig. 6. (Colour online) Snapshots of Dinobot walking on flat terrain.

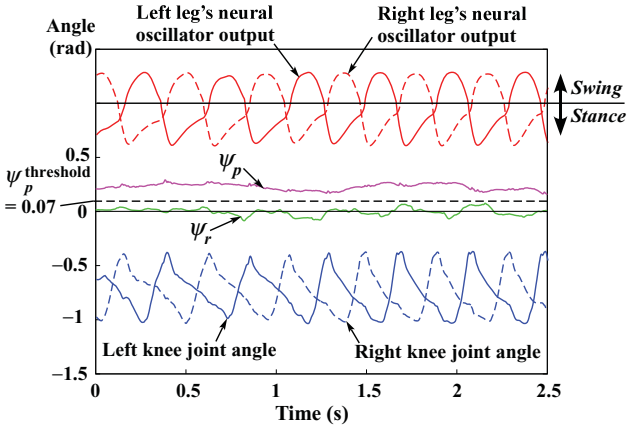


Fig. 7. (Colour online) Experimental result of Dinobot walking on flat terrain. The figure shows each leg's knee joint angle, the neural oscillator's output and the body inclination around the pitch and roll axes ($\psi_p$ and $\psi_r$). The origin and orientation of the knee joint angles and $\psi_p$ are shown in Figs. 3 and 4, respectively. $\psi_r$ is initialized in a vertically standing state and the sign is positive when the body inclines to the right side. In terms of each neural oscillator's output, if it is positive or negative, then the leg phase is swing or stance, respectively, as shown at the top. The threshold, $\psi_p^{\text{threshold}}$, which triggers the stepping reflex (Section 4.1.3), is empirically determined as 0.07.

In Fig. 8, the shape of the plot is irregular, but each cyclic trajectory is periodic and follows an almost fixed path. This means that the plot forms a limit cycle, and Dinobot's dynamic walking is stable as a nonlinear dynamic system. Therefore, we conclude that stable 3D dynamic walking has been achieved. Dinobot was capable of walking up to 7 m (approximately 35 steps) on flat terrain within a limited area because of the tether. However, Dinobot became strongly stable once the trajectory converged on the limit cycle. A longer distance would be expected.

### *5.2. Walking over a step*

To validate the effectiveness of the second mathematical feature of nonlinear oscillators in our system, an experiment to cross a step was conducted on a floor where we placed a step (height 15 mm (3.75% of leg length) and depth 120 mm). The experimental result is shown in Fig. 9. In this experiment, the walking speed was 1.2 m/s, the walking cycle period was 0.39 s, *Fr* was 0.61, the step was 0.2 m, which is much longer than the foot length (0.09m) and the duty factor was 0.55.

Letter A in Fig. 9 denotes the peak of the right knee joint angle at around 1.4 s and is observed to be lower than other peaks. This is because while swinging forward, the right leg touched the top of the step and landed on the step. As the foothold was more backward than usual, the body inclined forward around the pitch axis (towards the negative side) as indicated by letter B. If Dinobot had not reacted to this, it would have inclined significantly and fallen down. However, immediately after the body pitch inclination became smaller than the stepping reflex threshold ($\psi_p^{\text{threshold}} = 0.07$ rad) in C, the stepping reflex was activated and the leg was swung forward by the maximum possible amount

https://doi.org/10.1017/S0263574713001045 Published online by Cambridge University Press

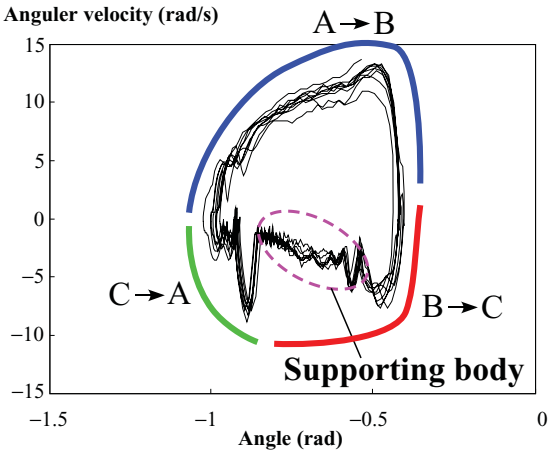


Fig. 8. (Colour online) A phase plane trajectory composed of measured right knee angle and angular velocity of Dinobot walking on flat terrain. In Fig. 8, points A, B and C correspond to those in Fig. 3. C→A is the period of lifting the leg backward, A→B is the period of swinging it forward and B→C is the period of supporting the body and obtaining propulsion. The duration of the dotted ellipse indicates the duration when the leg touches the ground and supports the body.

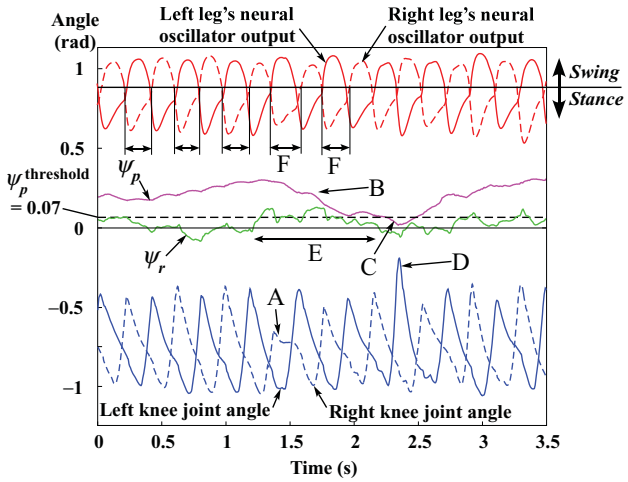


Fig. 9. (Colour online) Experimental result of Dinobot crossing a step. This figure is similar to Fig. 7, but it shows what happened when the robot reached the step at point A and after it successfully crossed over the step.

as denoted by point D in the figure. As a result, the body gradually inclined backward and did not fall down. Moreover, we can observe that when Dinobot landed on the step, the body inclined in the lateral plane as shown by point E (towards the positive side) as well as in the sagittal plane. Then, because of the effect of VSR (Section 4.2), the time period in which the right leg's neural oscillator output is negative, that is, the stance phase, became slightly longer than usual as indicated by point F. Thus, Dinobot supported its right leg for a longer duration than usual, and it can be observed that the body roll inclination ($\psi_r$) was gradually returning to its normal state. We can observe that Dinobot finally stabilized owing to the self-stabilization of neural oscillators.

In order to cross a step more than 15-mm high, Dinobot has to lift its feet high and adapt to body inclinations that occur when the single foot lands on a high obstacle. For the first task, the desired positions A and B in the swing phase (Fig. 3) should be raised. Specifically, ($\theta_{dA}$, $\phi_{dA}$, $k_{phA}$, $k_{paA}$) and ($\theta_{dB}$, $\phi_{dB}$, $k_{phB}$, $k_{paB}$) in Table I(b) are tuned. This can prevent the foot from catching on a tall obstacle, and therefore if Dinobot steps across a step, it can walk without falling. However, when the leg lands on a high step, the body oscillations around the pitch and roll axes occur. Although Dinobot is capable of adapting to the pitch oscillation with the stepping reflex (Fig. 4), it cannot adapt to a

https://doi.org/10.1017/S0263574713001045 Published online by Cambridge University Press

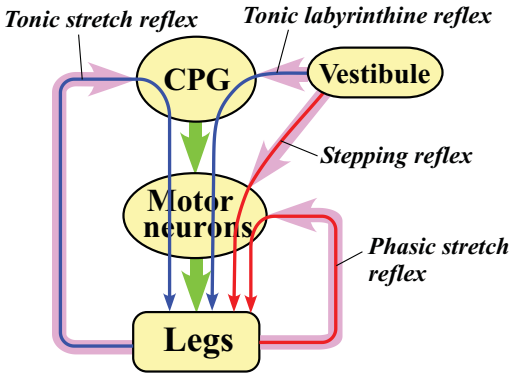


Fig. 10. (Colour online) An animal's nervous system. The reflex to adjust the leg rhythm via the neural oscillator (CPG) with time constants is called a tonic reflex: the tonic stretch reflex and the tonic labyrinthine reflex. The reflex to momentarily adjust the leg trajectory is called a phasic reflex: the stepping reflex and the phasic stretch reflex.

large roll oscillation (more than approximately $\pm 0.18$ rad). In order to adjust the state, Dinobot would have to use its tail or step sideways.

## 6. Discussion

Dinosaurs did not walk on perfectly flat terrain but over terrain that was many times slightly inclined and rugged. Moreover, while turning and performing rapid motions using their distinctive long tails, their leg trajectories and rhythms must have been as disturbed as that while walking over rough terrain. The previous conventional approaches to modelling their motion (where researchers attempted only to achieve a dinosaur's walking straight on flat terrain with a fixed leg trajectory and rhythm) are inherently insufficient for dynamic walking. Therefore, we consider that their nervous systems can adapt to disturbances in various walking situations.

### *6.1. Leg trajectory control by phasic reflexes and leg rhythm control by tonic reflexes*

We believe that dynamic walking is accomplished through 'leg trajectory control' and 'leg rhythm control' depending on the walking state on the basis of a neurophysiological study.[4] As shown in Fig. 10, the effect of the leg trajectory control activated by the stepping reflex (Section 4.1.3) momentarily appears via a motor neuron, and therefore we consider the stepping reflex to be a phasic reflex.[16] On the other hand, because the effect of the leg rhythm control activated by the tonic labyrinthine reflex (Section 4.2) appears to be slightly delayed via neural oscillator with time constants, the tonic labyrinthine reflex is considered to be a tonic reflex.[16] In the experiment discussed in Section 5.2 that involved walking over uneven terrain, when the body was inclined significantly, the swinging trajectory was adjusted forward by the stepping reflex and Dinobot immediately broke the fall; moreover, the disturbed leg rhythm after landing on the step was modified by the tonic stretch reflex and the tonic labyrinthine reflex. It has been proved that animals control their posture via various phasic and tonic reflexes that are activated by somatosensory and vestibular information.[11] In the future, we will incorporate other appropriate phasic and tonic reflexes so that Dinobot can adapt to various walking situations.

### *6.2. Control parameters tuning and its sensitivity*

The parameter values of the neural oscillators and the PD controllers in Table I were determined experimentally.

When we tuned all the parameters, we first set neural oscillators' parameters, next PD controllers' parameters were decided to make legged trajectories. Finally, we adjusted the oscillators' parameters, $k_{tsr}$ and $k_{vsr}$, to synchronize the oscillations of each oscillator and leg. In terms of the decision of the neural oscillators' parameters, the output of each neural oscillator is utilized for only phase switching (swing/stance phases), and we considered that it is most important to set the oscillator's cyclic duration, which is equivalent to the walking cycle duration. The cyclic duration of Matsuoka's

https://doi.org/10.1017/S0263574713001045 Published online by Cambridge University Press

neural oscillator[31] is decided by the proportion of $\tau$ to $\tau'$ in Eq. (1). In our experiments, $\tau/\tau'$ was set to 0.1 as shown in Table I in order to show that the walking cycle duration resulted in approximately 0.4 s, which was decided based on animals that have similar leg length. However, the walking cycle duration was slightly adjusted autonomously by walking with the synchronization of the oscillator, the leg and the body via the sensory feedbacks of Eqs. (3) and (6).

Here we discuss the sensitivities of the parameters. We experimentally observed a margin of error of each single parameter in Table I where Dinobot was capable of walking on flat terrain with more than 20 steps, which was recorded in the experiment in Section 5.1. Since the output of each neural oscillator is used for only phase switching, the parameters are flexible. However, the coefficients of sensory feedbacks, $k_{tsr}$ and $k_{vsr}$, are sensitive. The stable walking allows a margin of error of only approximately $\pm 3\%$. These are the parameters to synchronize the oscillations of each oscillator, each leg and the body. For this, we should set the parameters sensitively. The sensitivities of the desired angles in Table I(b) vary according to the desired positions A, B and C. Position A is the desired position only to lift the foot in order for the foot not to be obstructed while swinging forward from position A to B, each of the desired angles $\theta_{dA}$ and $\phi_{dA}$ allows a margin of error of approximately $\pm 15\%$. Position B, which is the end of swinging forward, is also the start of swinging backward, and thus it affects the touchdown angle, which is the hip angle at the moment when the foot touches the ground. The touchdown angle plays a significant role in the walking stability,[23] and $\theta_{dB}$ and $\phi_{dB}$ are sensitive. These are allowed in approximately $\pm 5\%$. The desired position C is also sensitive because it affects the touchdown angle and the propulsion. $\theta_{dC}$ and $\phi_{dC}$ are allowed in approximately $\pm 4\%$ and $\pm 6\%$, respectively. The P-gains have a similar tendency to the desired angles. $k_{phA}$ and $k_{paA}$ are allowed in approximately $\pm 20\%$, while $k_{phB}$, $k_{phC}$, $k_{paB}$ and $k_{paC}$ are merely allowed in approximately $\pm 9$, $\pm 6$, $\pm 12$ and $\pm 6\%$, respectively. All of the D-gains of the joints in every state are insensitive and changeable from approximately 0.005 to 0.03. This is because the D-gains are much smaller than the joints' friction and have small effects.

### *6.3. The probability of advanced walking using a tail*

A biped dinosaur's original mechanical structure is characterized by a long tail with a large moment of inertia. It has been reported that Deinonychus and Velociraptor made rapid movements by skillfully manipulating their tails.[13] Exploiting the tail enables rapid turning and movements but also causes perturbations that disturb the limit cycle for stable walking. This situation corresponds to that of walking over irregular terrain. Therefore, unless the rhythms of all body parts are synchronized at the same time, walking could not be achieved.

For example, when a dinosaur turns right by dynamically swinging the tail to the right side, the oscillations of the body parts are disturbed due to the loss of balance. The neural oscillators involving the tonic reflexes synchronize these disturbed oscillations, and smooth walking is achieved. The quadruped robot 'Tekken',[14] which used the biologically inspired method, sharply inclined its body towards the turning side by bending the leg joint of the same side, and subsequently lost its balance. However, because of the effect of its neural oscillators and tonic reflexes, Tekken could turn smoothly. Dinobot does not yet possess a tail joint. However, we believe that it has the potential to synchronize the oscillations disturbed by the tail movements because it has demonstrated to be capable of synchronizing disturbed oscillations in our experiments that involved walking over a step. Therefore, additional suitable tonic reflexes are required to significantly improve its synchronization capability. In addition, providing the tail's oscillation as feedback to the neural oscillator is an alternative idea.

## 7. Conclusions

In this paper, we have described stable dynamic walking of a biped dinosaur-like robot by means of the walking gait generation and control derived from an extant vertebrate's nervous system. First, we employed the basic neural system for locomotion of contemporary animals, which consists of CPG and spinal reflexes, for the dinosaur mimetic mechanism based on the knowledge derived from palaeontology and extant animals and appropriately tuned the parameters of the system empirically. As a result, we verified the generation of dynamic walking motion on flat terrain. Furthermore, we added reflexes (the stepping and vestibular spinal reflexes) dependent on a vestibule, similar to those

https://doi.org/10.1017/S0263574713001045 Published online by Cambridge University Press

in animals. We also demonstrated that our robot could robustly adapt to perturbations similar to animals while crossing a step. CPG can be one of the candidates that provides successful locomotion for a dinosaur.

Now we note some differences between the mechanism of Dinobot and that of dinosaurs as inferred from skeletal specimens. To increase its reliability, in the future, we will improve our model and make it more similar to actual skeletal specimens in terms of joint configuration and mass distribution of body parts among other features. In addition, until now, Dinobot has active joints only for its legs, but in our future work, we will exploit the motion of the long tail with a large moment of inertia, which is the dinosaurs' original feature, and accomplish turning and more advanced motion. Eventually, we would be pleased to discover a dinosaur's robust locomotive nervous system suitable for particular mechanism.

**Acknowledgements**

This work was supported by Ibaraki University (Life Support Project). We would like to thank Kazuyoshi Mori, Naoji Shiroma and Kosuke Inoue for their valuable comments and advice.

**References**

1. S. Aoi and K. Tsuchiya, "Adaptive behavior in turning of an oscillator-driven biped robot," *Auton. Robots* **23**(1), 37–57 (2007).
2. R. M. Alexander, "Optimization and gaits in the locomotion of vertebates," *Phys. Rev.* **69**, 1199–1227 (1989).
3. R. M. Alexander, *Dynamics of Dinosaurs and Other Extinct Giants* (Columbia University Press, New York, NY, 1989).
4. R. E. Burke, A. M. Degtyarenko and E. S. Simon, "Patterns of locomotor drive to motoneurons and last-order interneurons: Clues to the structure of the CPG," *J. Neurophysiol.* **86**, 447–462 (2001).
5. A. H. Cohen and D. L. Boothe, "Sensorimotor interaction during locomotion: Principles derived from biological system," *Auton. Robots* **7**(3), 239–245 (1999).
6. H. Franzen, "Walking the dinosaur," *Scientific American* (July 9, 2001).
7. Ö. Ekeberg and K. Pearson "Computer simulation of stepping in the hind legs of the cat: An examination of mechanisms regulating the stance-to-swing," *Trans. J. Neurophys.* **94**(6), 4256–4268 (2005).
8. G. Endo, J. Morimoto, J. Nakanishi and G. Cheng "An Empirical Exploration of a Neural Oscillator for Biped Locomotion Control, **In**: *Proceedings of the the 2004 IEEE International Conference on Robotics & Automation* (2004) pp. 3036–3042.
9. G. Endo, J. Nakanishi, J. Morimoto and G. Cheng "Experimental Studies of a Neural Oscillator for Biped Locomotion with QRIO," **In**: *Proceedings of the 2005 IEEE International Conference on Robotics and Automation* (2005) pp. 598–604.
10. K. Ezure and V. J. Wilson, "Interaction of Tonic Neck and Vestibular Reflexes in the Forelimb of the Decerebrate Cat," *Exp. Brain Res.* **54**(2), 289–292 (1984).
11. J. Fagard and P. H. Wolff, "The development of timing control and temporal organization in coordinated action invariant relative timing, rhythms and coordination," *Adv. Psychol.* **81**, 151–173 (1991).
12. Y. Fukuoka, H. Kimura and A. H. Cohen, "Adaptive dynamic walking of a quadruped robot on irregular terrain based on biological concepts," *Int. J. Robot. Res.* **22**(3–4), 187–202 (2003).
13. D. E. Fastovsky and D. B. Weishampel *The Evolution and Extinction of the Dinosaurs*. (Cambridge University Press, Cambridge, UK 2005).
14. Y. Fukuoka, H. Katabuchi and H. Kimura, "Dynamic locomotion of quadrupeds "Tekken3 & 4" using simple navigation," *J. Robot. Mechatronics* **22**(1), 36–42 (2010).
15. R. Full and D. E. Koditschek, "Templates and anchors: Neuromechanical hypotheses of legged locomotion on land," *J. Exp. Biol.* **202**, 3325–3332 (1999).
16. P. D. Gail, J. W. Lance and P. D. Neilson, "Differential effects on tonic and phasic reflex mechanisms produced by vibration of muscles in man," *J. Neurol. Neurosurg. Psychiat.* **29**(1), 1–11 (1966).
17. S. Gatesy, R. Kambic and T. Roberts, "Long-axis Rotation (LAR): A Missing Degree of Freedom in Avian Bipedal Locomotion," *Proceedings of Dynamic Walking 2012* (2012).
18. S. Grillner, "Control of Locomotion in Bipeds, Tetrapods and Fish," **In**: *Handbook of Physiology*, Vol. II (American Physiological Society, Bethesda, MD, 1981) pp. 1179–1236.
19. S. Grillner and P. Wallen, "On peripheral control mechanisms acting on the central pattern generators for swimming in the dogfish," *J. Exp. Biol.* **98**, 1–22 (1982).
20. L. Guan, T. Kiemel and A. H. Cohen, "Impact of movement and movement-related feedback on the Lamprey central pattern generator for locomotion," *J. Exp. Biol.* **204**, 2361–2370 (2001).
21. K. Hase and N. Yamazaki, "Computational evolution of human bipedal walking by a neuro-musculo-skeletal model," *Artif. Life Robot.* **3**, 133–138 (1988).

22. H. Hirukawa, F. Kanehiro, K. Kaneko, S. Kajita and M. Morisawa, "Dinosaur robotics for entertainment applications design, configuration, control, and exhibition at the world exposition," *IEEE Robot. Autom. Mag.* **14**(3), 43–51 (2007).
23. P. Holmes, R. J. Full, D. Koditschek and J. Guckenheimer, "The dynamics of legged locomotion: Models, analyses, and challenges," *Soc. Ind. Appl. Math.* **48**, 207–304 (2006).
24. F. Iida and R. Tedrake, "Minimalistic control of biped walking in rough terrain," *Auton. Robots* **28**, 355–368 (2010).
25. H. Kimura, Y. Fukuoka and A. H. Cohen, "Adaptive dynamic walking of a quadruped robot on natural ground based on biological concepts," *Int. J. Robot. Res.* **26**(5), 475–490 (2007).
26. S. Kotosaka and S. Schaal, "Synchronized Robot Drumming by Neural Oscillator," *Proceedings of the International Symposium on Adaptive Motion of Animals and Machines* (2000).
27. D. Lambert, *The Ultimate Dinosaur Book* (Dorling Kindersley, New York, NY, 1993).
28. G. Lee, R. Lowe and T. Ziemke, "Modelling Rarly Infant Walking: Testing a Generic CPG Architecture on the NAO Humanoid," *Proceedings of the IEEE Joint Conference on Development and Learning and on Epigenetic Robotics* (2011).
29. M. A. Lewis, F. Tenore and R. Etienne-Cummings, "CPG Design Using Inhibitory Networks," **In**: *Proceedings of the 2004 IEEE International Conference on Robotics & Automation* (2005) 3682–3687.
30. T. Matsubara, J. Morimoto, J. Nakanishi, M. Sato and K. Doya, "Learning CPG-based biped locomotion with a policy gradient method," *Robot. Auton. Syst.* **54**, 911–920 (2006).
31. K. Matsuoka, "Mechanisms of frequency and pattern control in the neural rhythm generators," *Biol. Cybern.* **56**, 345–353 (1987).
32. S. Miyakoshi, M. Yamakita and K. Furuta, "Juggling Control Using Neural Oscillators," **In**: *Proceedings of the IEEE/RSJ International Conference on Intelligent Robots and Systems* (1994) pp. 1186–1193.
33. J. Nakanishi, J. Morimoto, G. Endo, G. Chenga, S. Schaal and M. Kawato, "Learning from demonstration and adaptation of biped locomotion," *Robot. Auton. Syst.* **47**(2–3), 79–91 (2004).
34. D. J. Ostry, P. L. Gribble, M. F. Levin and A. G. Feldman, "Phasic and tonic stretch reflexes in muscles with few muscle spindles: Human jaw-opener muscles," *Exp. Brain Res.* **116**, 299–308 (1997).
35. G. S. Paul, *Predatory Dinosaurs of the World*. (Simon and Schuster, York City, NY, 1988).
36. K. G. Pearson and R. Franklin, "Characteristics of leg movements and patterns of coordination in locusts walking on rough terrain," *Int. J. Robot. Res.* **3**(2), 101–112 (1984).
37. G. Hiebert, M. Gorassini, W. Jiang, A. Prochazka and K. Pearson, "Corrective responses to loss of ground support during walking II, comparison of intact and chronic spinal cats," *J. Neurophys.* **71**(2), 611–622 (1994).
38. E. H. Pelc, M. A. Daley and D. P. Ferris "Resonant hopping of a robot controlled by an artificial neural oscillator," *Bioinspir. Biomim.* **3**, 260–261 (2008).
39. B. I. Polus, A. Patak, J. E. Gregory and U. Proske, "Effect of muscle length on phasic stretch reflexes in humans and cats," *J. Neurophys.* **66**(2), 613–622 (1991).
40. M. Robin *A Physiological Handbook for Teachers of Yogasana* (Fenestra Books, Tucson, AZ, 2002).
41. W. I. Sellers and P. L. Manning, "Estimating dinosaur maximum running speeds using evolutionary robotics," *Proc. Royal Soc. B* **274**(1626), 2711–2716 (2007).
42. M. L. Shik and G. N. Orlovsky, "Neurophysiology of locomotor automatism," *Phys. Rev.* **56**(3), 465–501 (1976).
43. G. S. Stent, W. B. Kristan, Jr., W. O. Friesen, C. A. Ort, M. Poon and R. L. Calabrese, "Neuronal generation of the leech swimming movement," *Science* **200**(4348), 1348–1357 (1978).
44. G. Taga, Y. Yamaguchi and H. Shimizu, "Self-organized control of bipedal locomotion by neural oscillators," *Biol. Cybern.* **65**, 147–159 (1991).
45. K. Takita, T. Katayama and S. Hirose, "Development of Miniature Dinosaur-Like Robot TITRUS-III," **In**: *Proceedings of 2001 IEEE/RSJ International Conference on Intelligent Robots and Systems* (2001), pp. 852–857.
46. K. Tsujita, T. Inoura, A. Morioka, K. Nakatani, K. Suzuki and T. Masuda, "Oscillator-controlled bipedal walk with pneumatic actuators," *J. Mech. Sci. Technol.* **21**(3), 976–980 (2007).
47. M. M. Williamson, "Neural control of rhythmic arm movements," *Neural Netw.* **11**(7–8), 1379–1394 (1998).